Kinetic study and characterization of the Wittig reaction between 4-(nitrobenzyl) triphenylphosphonium bromide, potassium hydroxide (KOH) and benzaldehyde

Emily Abplanalp[a], Zachary Dwyer[a], Maya Florentino[a], Kristen Mardenborough[a]

[a] *Department of Materials Science and Chemical Engineering, Stony Brook University, Stony Brook, NY 11794, USA*

Abstract:

The flexibility and vast applicability of the Wittig reaction have led to extensive analysis to understand its underlying mechanism. Applications of the Wittig reaction extend to vitamin syntheses and pharmaceutical production. The general mechanism follows the reaction of a phosphonium ylide with an aldehyde or ketone to produce an alkene and phosphine oxide. A phosphonium salt is used to create the ylide, which is formed using a base. In this study, a prototypical experiment involving 4-(nitrobenzyl) triphenylphosphonium bromide (NBTP) and potassium hydroxide (KOH) was performed to form the ylide, and the Wittig reaction was initiated via the addition of benzaldehyde. The ylide formed is red in color, and the mixture decolorized to yield a colorless solution after benzaldehyde addition. The pseudo reaction order was investigated for the disappearance of the ylide. UV-visible spectroscopy was used to track the progression of the reaction, which was found to be first-order with respect to the ylide. Characterization of both the ylide and product was completed using Fourier-transform infrared (FTIR) and Raman spectroscopy.

Keywords: Wittig reaction, kinetics, ylide, Raman spectroscopy, Fourier-transform infrared spectroscopy, UV-visible spectroscopy

1. Introduction

Known for its wide range of applications and versatility, the Wittig reaction is used in organic syntheses and especially in the manufacturing of vitamins and pharmaceuticals [1,2]. The general mechanism consists of a carbonyl group from an aldehyde or ketone reacting with a phosphonium ylide to create a mixture of cis- and trans-alkenes [3]. A phosphonium salt can be used to create the ylide, which must be formed using a base. This reaction has been used in introductory university organic chemistry laboratories to teach students about an important step that is present in many syntheses [4,5].

The Wittig reaction is typically used as a one-step process within a complex synthesis to create a product. It is a key step in the synthesis of lavendamycin ethyl ester, a compound known for its antimicrobial and antitumor properties [6]. Otero et al. employed the highly stereoselective nature of the Wittig reaction to synthesize retinoids, which are vital for mammal reproduction, cell growth, and immune system strength [7]. The Wittig reaction is also involved in the synthesis of α-tocopherol, a form of vitamin E known for its antioxidant properties and ability to prevent degenerative neuropathy [8].

Although the usefulness of the Wittig reaction has been extensively explored, commercial uses for this reaction tend to be unsustainable and hazardous, utilizing toxic chemicals such as lithium-based solvents. Alternative solvents and the use of water as a medium have been researched. Dambacher et al. found that the use of water for a variety of stabilized ylides and aldehydes resulted in faster reaction rates and higher product yields when compared to conventional methods [9]. Solvent-free approaches have also been investigated using catalysts (e.g., MnO_2 for doping MgO nanocomposites) [10].

In this study, we analyzed the reaction between 4-(nitrobenzyl) triphenylphosphonium bromide (NBTP), potassium hydroxide (KOH) and benzaldehyde using ethanol as a solvent. Figure 1 shows the potential mechanism for this reaction based on the generally accepted mechanism involving the formation of oxaphosphetane as the only intermediate. Ylide formation and disappearance were tracked using the characteristic red color shown in Figure 2. When benzaldehyde was added to the solution, the color faded, indicating the progression of the reaction. Using UV-visible (UV-vis) spectroscopy, we performed a

kinetic study to determine the pseudo reaction order with respect to the ylide disappearance for the Wittig reaction in excess benzaldehyde. Characterization of the formed ylide and product was completed using Raman spectroscopy and Fourier-transform infrared (FTIR) spectroscopy.

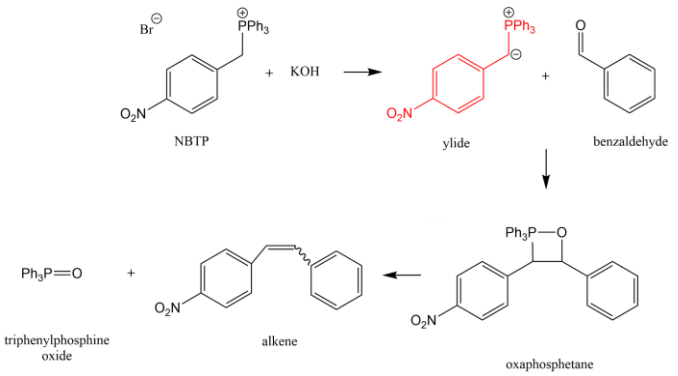

Figure 1. Proposed formation of the red ylide using NBTP and KOH followed by the addition of benzaldehyde to form an alkene and triphenylphosphine oxide adapted from the mechanism proposed by Skelton et al. [11] (figure rendered using PerkinElmer Informatics ChemDraw (20.1)).

Because the Wittig reaction is widely used in the pharmaceutical industry, understanding of the mechanism is crucial for the development of new biologic and chemotherapeutic agents. Current Wittig reactions employed for pharmaceutical production often include hazardous reactants, byproducts, and reaction conditions. To establish green chemistry models for alternate, environmentally safer processes, a wealth of kinetic data currently undiscovered must be further investigated. Our study seeks to characterize common species involved in Wittig reactions and their kinetic parameters to make way for future modeling of green alternatives for the use of Wittig reactions in pharmaceutical manufacturing.

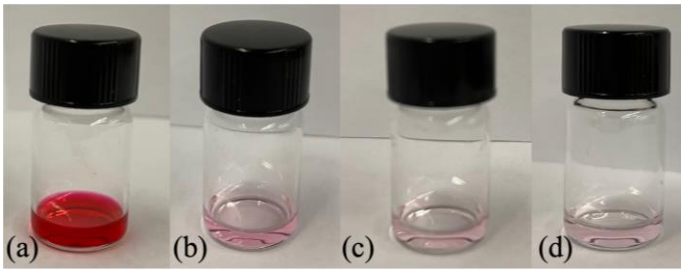

Figure 2. Reaction progression for 40 min. (a) initial mixing of 0.01 M KOH and 0.01 M NBTP, (b) NBTP and KOH solution after 20 min, (c) initial addition of 0.10 M benzaldehyde at 20 min, (d) final solution after 40 min (20 min after adding benzaldehyde).

2. Materials and Methods

2.1 Sample Preparation

For preparation of a 0.10 M stock NBTP solution, 9.56 mg of NBTP powder was dissolved in 10 mL of 200 proof anhydrous ethyl alcohol (ethanol) (ACROS, CAS#: 64-17-5) using a magnetic stir bar and stir plate. The solution was stirred at 300 rpm without heating for 30 minutes, at which point the solution was observed to be clear and fully dissolved. Subsequent serial dilutions of the stock were utilized for the creation of 10×10^{-3} M, 7.50×10^{-3} M, 5.00×10^{-3} M, 3.75×10^{-3} M, and 2.50×10^{-3} M NBTP samples. A stock solution of 0.20 M KOH solution was prepared similarly by dissolving 111.3 mg of KOH pellets (GBiosciences, CAS#: 1310-58-3) in 10 mL of ethanol using a magnetic stir bar and stir plate. This solution was stirred at 300 rpm without heating until the pellets were fully dissolved. A serial dilution of 0.01 M KOH solution was created from the initial stock solution. A working solution of 0.10 M benzaldehyde was made from a 9.8 M liquid Benzaldehyde ReagentPlus® (SIGMA-ALDRICH, CAS#: 100-52-7) stock solution and diluted with ethanol.

2.2 Standard Curve

A standard curve for the ylide was created using a 0.01 M KOH solution with NBTP concentrations of 2.50×10^{-3} M, 3.75×10^{-3} M, 5.00×10^{-3} M, 7.50×10^{-3} M, and 10×10^{-3} M. The NBTP samples were first pipetted in volumes of 50 µL into a 96-well microplate (Corning Falcon 351172 STERILE R). Aliquots of 50 µL 0.01 M KOH were added to each well and data was collected 20 min after the start of each reaction for the curve. The samples were analyzed using a Tecan Infinite 200 PRO UV-visible spectrophotometer at the characteristic wavelength of 515 nm with 2 flashes for 20 min. The calibration curve is displayed in Figure S1.

2.3 Rate Law Investigation

UV-vis spectra were obtained via a Tecan Infinite 200 PRO UV-visible spectrophotometer. The samples were pipetted in total volumes of 100 µL into a microplate (96 well Corning Falcon 351172 STERILE R), and measurements were conducted at room temperature in the range of 400-700 nm with a step size of 5 nm, and 2 flashes. All absorbance data was recorded using the i-control™ Microplate Reader Software 1.11 (for Infinite reader).

Analysis with UV-vis spectroscopy was performed using 0.01 M NBTP, 0.01 M KOH and 0.10 M benzaldehyde. Triplicate wells were used for each sample concentration. The NBTP samples were first pipetted in

volumes of 47.2 µL into the microplate. Following NBTP addition, KOH samples of 47.2 µL were then added via the same procedure to each well to initiate ylide formation. After a period of 20 min, 5.6 µL of 0.10 M benzaldehyde was pipetted into each well, initiating the formation of the product. The samples were then analyzed using UV-vis for 20 min after the addition of benzaldehyde in 1 min increments.

2.4 Characterization

The infrared spectra were obtained with a Nicolet iS50 FTIR spectrometer (Thermo Fisher Scientific) equipped with an attenuated total reflectance (ATR) accessory. The samples were contacted with a diamond ATR crystal and FTIR spectra (32 scans) were collected between 400~4000 cm^{-1} with a resolution of 4 cm^{-1}. An ethanol background was used for the ylide, product, and 0.01 M NBTP spectra. An air background was used for the benzaldehyde stock solution spectrum.

To prepare the ylide and product samples for FTIR spectroscopy, 0.01 M NBTP, 0.01 M KOH, and 0.10 M benzaldehyde solutions (1:1:10 stoichiometric ratio) diluted in ethanol were used. For each sample, 0.01 M NBTP and 0.01 M KOH were combined in a scintillation vial, which was capped and stored on the benchtop for 20 min to allow the solution to reach equilibrium. An ylide absorbance spectrum was then collected with an ethanol background. For the product sample, 0.10 M benzaldehyde was added to the vial. The scintillation vial was then capped and stored on the benchtop for an additional 20 min, after which an absorbance spectrum for the alkene product was then collected.

Near-infrared Raman spectra of samples were obtained using a Horiba-Jobin XploRATM Raman spectrometer (785 nm). The exposure and accumulation times were 10 seconds and 20 scans, respectively. The power was set to 25%. Before collecting the Raman spectra of the sample, the spectrometer was calibrated via silicon material using a 100× objective and a 1200 gr/mm grating. The Raman spectra were collected in the 200~2000 cm^{-1} Raman shift region.

Ylide and product samples used for Raman spectroscopy were prepared with 0.05 M NBTP, 0.05 M KOH, and 0.5 M benzaldehyde (1:1:10 stoichiometric ratio). These solutions were prepared by diluting the stock solutions with ethanol. For each sample, 236 µL of 0.05 M NBTP and 236 µL of 0.05 M KOH were pipetted into 2 mL scintillation vials and capped to prevent the evaporation of ethanol. The solution was kept on the benchtop for 20 min to allow the ylide to form. Afterwards, a micropipette was used to move the solution from one vial to a flat glass dish for the ylide sample. The dish was placed in a fume hood to promote the rapid evaporation of ethanol. For the product sample, after 20 min on the benchtop, 28 µL of 0.5 M benzaldehyde was added to the vial, which was capped and left on the benchtop for another 20 min. After this time, the product sample was poured into a glass dish and left in the fume hood. Raman spectra were collected 4 days later.

3. Results and Discussion

3.1 *Kinetic Study*

The study that prompted our research into this reaction stemmed from an article produced by Corning Incorporated [12]. Using UV-vis, we observed that the only peak in the spectra occurred at 515 nm when NBTP and KOH were combined to form the ylide. The spectra obtained from the NBTP, KOH, and benzaldehyde stock solutions did not show any peaks near 515 nm.

Figure 3 displays the progression of the reaction using the data reported for Figures 4-6 showing the zero-, first-, and second-order plots for 0.01 M NBTP, 0.01 M KOH, and 0.10 M benzaldehyde. The reaction seems to be first-order, as this plot shows the best linearity. Following the benzaldehyde addition, a period of 3 min was allotted prior to data collection to allow settling of the samples and warming of the spectrophotometer. Upon the start of data collection, absorbance values reflected ~40% conversion of the ylide into the alkene product.

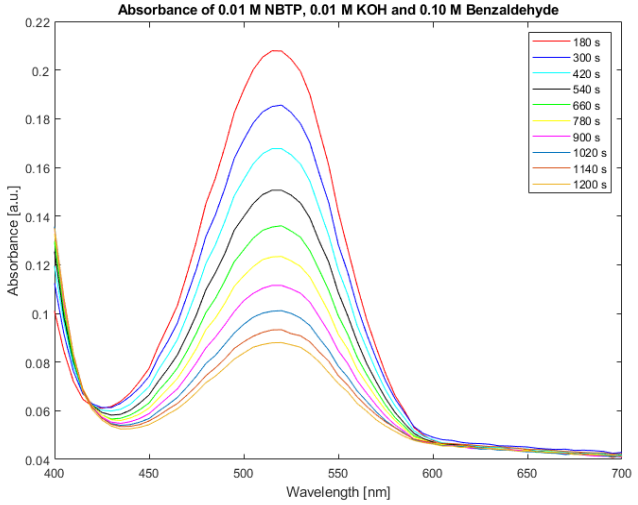

Figure 3. UV-visible spectra for the reaction between 0.01 M NBTP, 0.01 M KOH, and 0.10 M benzaldehyde.

3.2 *Fourier-Transform Infrared Spectroscopy (FTIR)*

FTIR was used to identify the characteristic vibrational spectroscopic peaks in the reagents, ylide, and final product. The spectrum of 0.01 M KOH in ethanol was omitted as it lacks any characteristic peaks aside from the O-H stretching between 3000~3500 cm^{-1} [13].

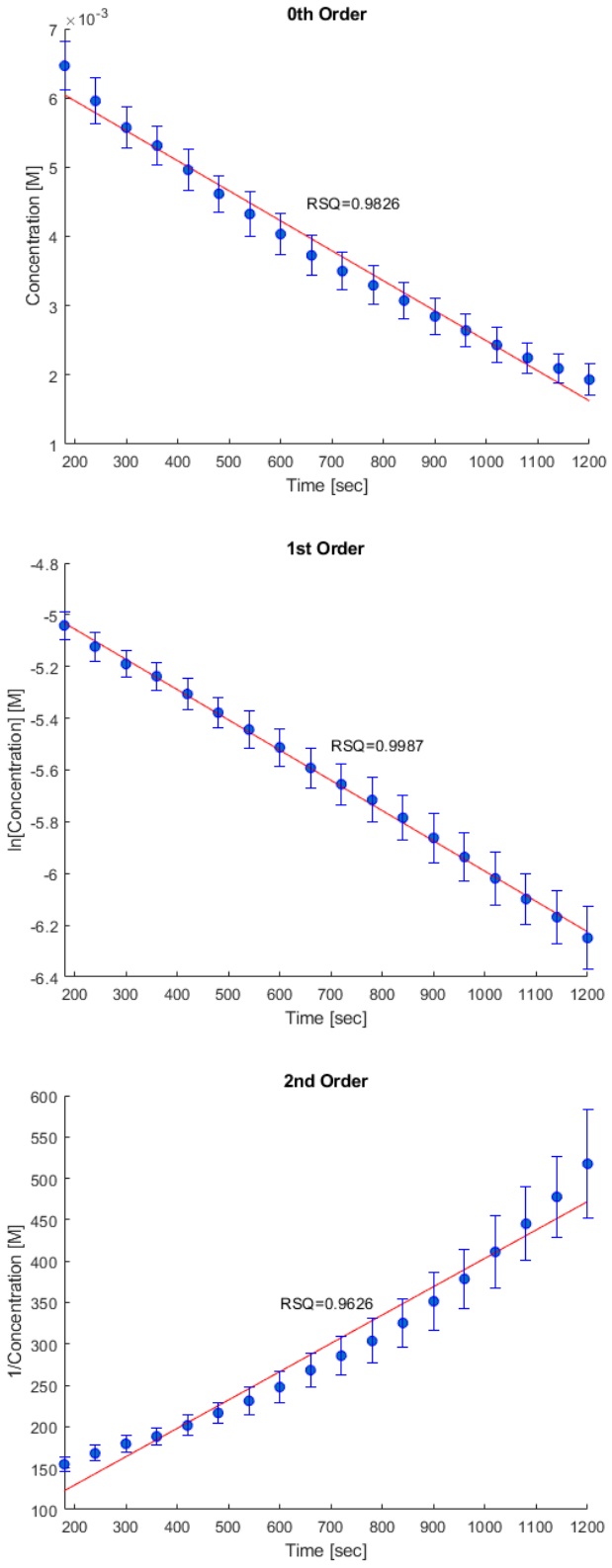

Figures 4-6. Reaction order plots for the reaction between 0.01 M NBTP, 0.01 M KOH, and 0.10 M benzaldehyde. Ylide formation was allowed to proceed for 20 min before the addition of benzaldehyde.

The FTIR spectra of 0.10 M NBTP, the ylide, and the product were all measured with an ethanol background. This was done to minimize the intensity of the ethanol peaks. Since the ethanol was not fully subtracted, some peaks are still present such as C-O stretching at 1049 cm^{-1} and 1092 cm^{-1}, and C-H bending at 881 cm^{-1} [14]. The benzaldehyde spectrum has positive absorbance values since the stock solution measured did not contain ethanol.

Analysis of the FTIR spectra was conducted to compare the phosphonium ylide to NBTP. The ylide is formed through reduction of NBTP; therefore, the ylide contains a carbanion. Due to this minor conformational change in structure from NBTP to the ylide, the FTIR spectra appear identical as seen in Figure 7. Although the FTIR data indicate that this change was not detected, the visual color change of the solution confirms the ylide formation. Characteristic peaks shared by the absorbance spectra of NBTP and the ylide include those associated with bending and stretching of C-O bonds (1049 cm^{-1}, 1090~1092 cm^{-1}, 1375~1377 cm^{-1})and C-H bonds (1657-1659 cm^{-1} [aromatic bending], 2870~2872 cm^{-1}, 2924 cm^{-1}, 2970~2972 cm^{-1}), with an additional peak representing the nitro group present in both compounds (1348~1350 cm^{-1}) [13,15].

After the ylide formed, benzaldehyde was added to create the alkene product. As seen in Figure 7, two characteristic peaks present in the benzaldehyde spectrum are absent in the product spectrum. The peak at ~1696 cm^{-1} corresponds to C=O stretching, which is found in the benzaldehyde structure only [16]. Another characteristic peak found only in the benzaldehyde spectrum is at ~1203 cm^{-1} corresponding to both aldehydic C-H bending and C=C stretching [16]. A peak at ~1348 cm^{-1} is found in the product but not in the benzaldehyde spectrum and corresponds to the nitro group present in the product [13].

3.3 Raman Spectroscopy

Following the procedures described in the experimental section, we prepared the ylide and product. These samples, along with samples of the reagents used, were excited with a 785 nm laser to collect the Raman spectra (Figure 8). In the 200~2000 cm^{-1} region, it is easily observed that KOH did not show any distinguishable peaks. Peaks that were unique to benzaldehyde include those at 439 cm^{-1}, 829 cm^{-1}, and 1594 cm^{-1}, corresponding to C_4C_7/C_3C_4 stretching or $C_2C_3C_4$ bending within the phenyl ring, C_4C_7 stretching or $C_1C_2C_6$ bending, and C-C stretching within the phenyl ring [17,18]. All samples except for KOH displayed peaks from 615~617 cm^{-1}, corresponding to bending of the phenol groups [19].

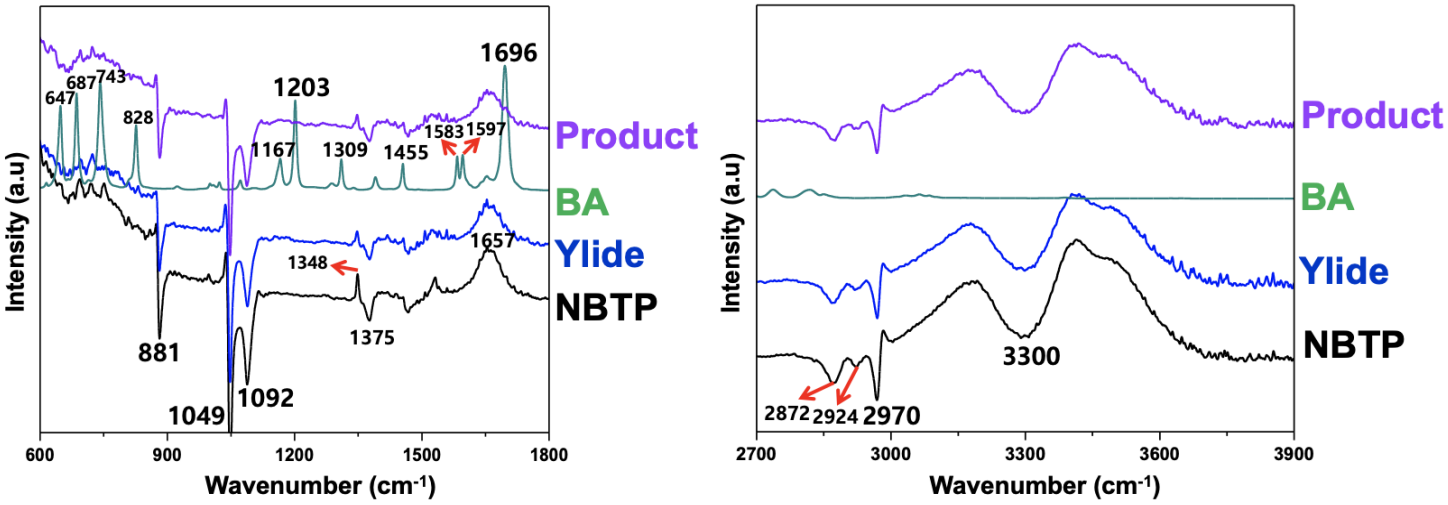

Figure 7. FTIR spectra of the final product, benzaldehyde stock solution (BA), ylide, and 0.01 M NBTP.

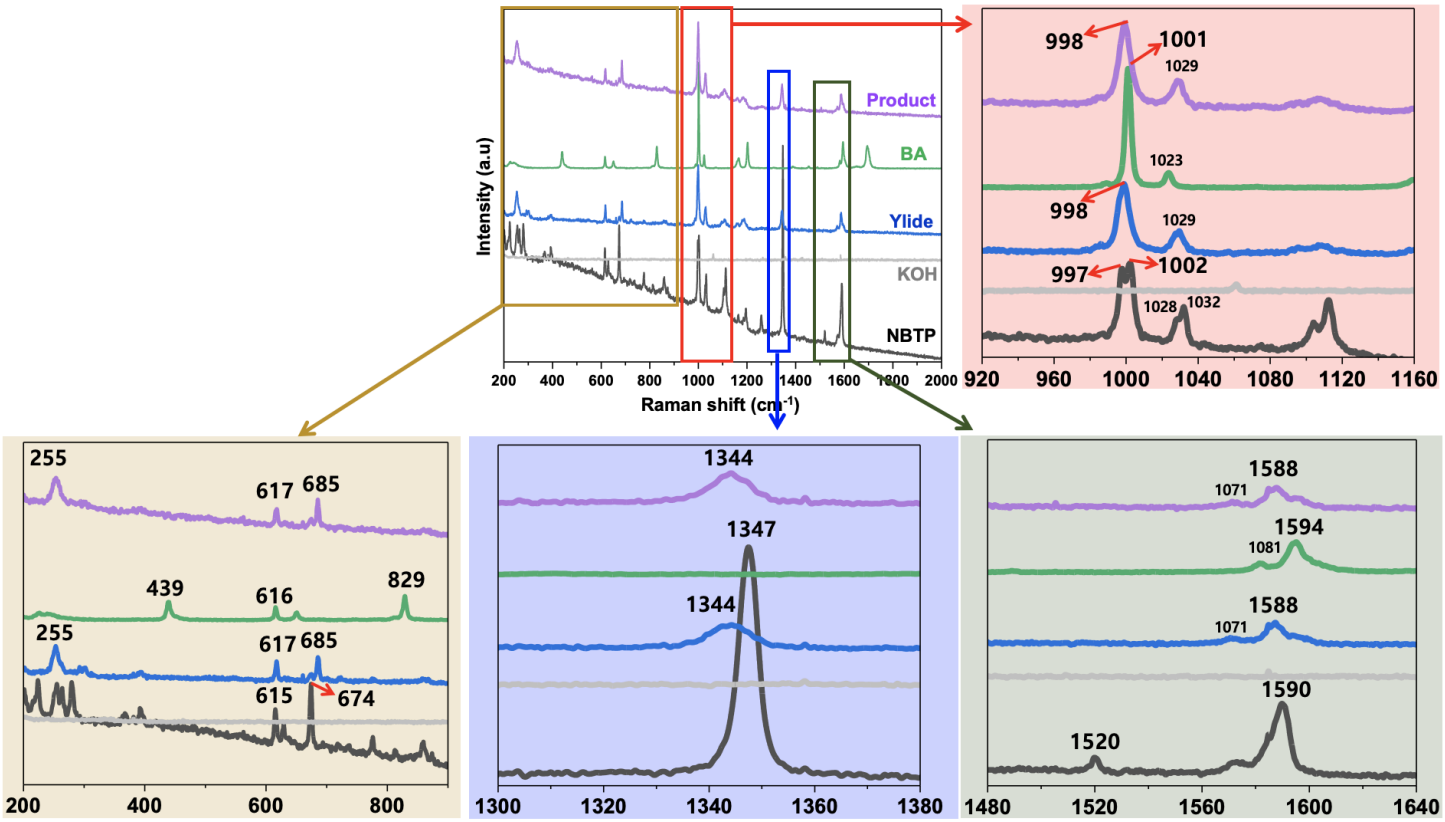

Figure 8. Raman (785 nm excitation wavelength) spectra of the product, benzaldehyde (BA), ylide, KOH, and NBTP. Highlighted regions in the Raman shift region of 200~2000 cm^{-1} include 200~900 cm^{-1} (yellow), 920~1160 cm^{-1} (red), 1300~1380 cm^{-1} (blue), and 1480~1640 cm^{-1} (green).

Peaks at 255 and 685 cm^{-1} are present for the product, ylide, and NBTP. These peaks are assigned to C-P-C deformation and C-P stretching, respectively [20,19]. The product, ylide, and NBTP show peaks at 1028~1029 and 1588~1590 cm^{-1}, displaying deformation vibration of C-H on phenyl [19] and C-C or C-N stretching [20], respectively. Additionally, there are peaks present in the region of 997~1002 cm^{-1}; however, these peaks are difficult to characterize as the NBTP spectrum clearly shows two peaks in this region. These peaks may be the result of the skeletal vibration mode of the aromatic carbon atoms [19,21]. In the 1300~1380 cm^{-1} region, a strong peak is present at 1347 cm^{-1} in the NBTP spectrum while relatively weak peaks are shown at 1344 cm^{-1} for the product and ylide. The shift may be due to vibrations in aromatic moieties of NBTP [20]. No peaks were observed that correlated to C=C in the alkene product spectrum.

3.4 Discussion

From Figures 7 and 8, it is apparent that the FTIR and Raman spectra for both the product and ylide are similar. We believe this may result from several causes, including low yield of ylide and product samples due to low reagent concentrations and the structural similarity of the species.

Cis-alkene formations lack a characteristic peak due to probable overlap of the alkene peaks with those of the cis double bonds within the ring structures of the reagents and ylide. Characteristic peaks of the product that would help distinguish between the two species would be the P=O bond in the triphenylphosphine oxide and the trans-alkene bond. P=O stretching is typically present at ~1191 cm^{-1} and between 1250-1350 cm^{-1} in FTIR spectra [14,22,23]. Further, for a trans-alkene, trans C-H out-of-plane bending is found between 960-970 cm^{-1} and the double bond has characteristic peaks at 990 cm^{-1} and 775 cm^{-1} [14,24,25]. In the Raman spectra, C=C stretching should be seen around 1670 cm^{-1} [26,27].

Though it may be difficult to recognize product formation in the FTIR and Raman spectra, based on the kinetic data it is evident that the ylide was converted into the product as the absorbance values in Figure 3 decrease over time, indicating disappearance of the ylide. In order to confirm the structure of the alkene bond and further characterize the ylide and product, future work with ^{1}H-NMR is strongly encouraged. The use of ^{1}H-NMR may be used to distinguish the nature of the alkene bond formed.

4. Conclusion

In this study, characterization of fundamental Wittig reagents, a phosphonium ylide, and the final product are reported for a standard Wittig reaction involving NBTP, KOH, and benzaldehyde in anhydrous ethanol. Subsequent reaction order investigations were performed, suggesting a first-order rate law for the disappearance of the ylide. To our knowledge, this is the first reported study characterizing a Wittig reaction using these reagents.

It is the authors' hope that this can serve as a basis for future work and modeling for greener Wittig alternatives. Verification of cis- and trans-alkene product yields via ^{1}H-NMR analysis and potential applications of the alkene product synthesized from the reported reaction between NBTP, benzaldehyde, and KOH should be explored.

5. Acknowledgements

We would like to thank Dr. Taejin Kim and Dr. Yizhi Meng for their continual support and advice throughout this project. Additionally, we would like to thank Dr. Taejin Kim for his assistance in collecting the Raman spectra, Dr. Yizhi Meng for providing us with the UV-visible spectrophotometer, and Dr. Rina Tannenbaum for the use of her FTIR and Raman instruments.

6. References

[1] D. H. A. Rocha, D. C. H. A. Pinto, and A. M. S. Silva, "Applications of the Wittig reaction on the synthesis of natural and natural-analogue heterocyclic compounds," *EurJOC*, pp. 2443-2457, 2018.

[2] K. Zhang, L. Q. Lu, and W. J. Xiao, "Recent advances in the catalytic asymmetric alkylation of stabilized phosphorus ylides," *ChemComm*, vol. 55, pp. 8716-8721, 2019.

[3] P. Farfán, S. Gómez, and A. Restrepo, "On the origins of stereoselectivity in the Wittig reaction," *Chem. Phys. Lett.*, vol. 728, pp. 153-155, August 2019.

[4] L. A. Morsch, L. Deak, D. Tiburzi, H. Schuster, and B. Meyer, "Green aqueous Wittig reaction: Teaching green chemistry in organic teaching laboratories," *J. Chem. Educ.*, vol. 91, pp. 611-614, February 2014.

[5] F. J. Robertson, "A highly versatile one-pot aqueous Wittig reaction," *World J. Chem. Educ.*, vol. 4, pp. 101-106, 2016.

[6] P. Molina, F. Murcia, and P. M. Fresneda, "A straightforward and practical formal synthesis of lavendamycin ethyl ester," *Tetrahedron Lett.*, vol. 35, pp. 1453-1456, February 1994.

[7] M. P. Otero, A. Torrado, Y. Pazos, F. Sussman, and A. R. de Lera, "Stereoselective synthesis of annular 9-cis-retinoids and binding characterization to the retinoid X receptor," *J. Org. Chem.*, vol. 67, pp. 5876-5882, July 2002.

[8] T. Muller, D. Coowar, M. Hanbali, P. Heuschling, and B. Luu, "Improved synthesis of tocopherol fatty alcohols and analogs: microglial activation modulators," *Tetrahedron*, vol. 62, pp. 12025-12040, December 2006.

[9] J. Dambacher, W. Zhao, A. El-Batta, R. Anness, C. Jiang, and M. Bergdahl, "Water is an efficient medium for Wittig reactions employing stabilized ylides and aldehydes," *Tetrahedron Lett.*, vol. 46, pp. 4473-4477, June 2005.

[10] M. H. Moulavi, B. B. Kale, D. Bankar, D. P. Amalnerkar, A. Vinu, and K. G. Kanade, "Green synthetic methodology: An evaluative study for impact of surface basicity of MnO_2 doped MgO

nanocomposites in Wittig reaction," *J. Solid State Chem.*, vol. 269, pp. 167-174, January 2019.

[11] V. Skelton, G. M. Greenway, S. J. Haswell, P. Styring, D. O. Morgan, B. Warrington, and S. Y. F. Wong, "The preparation of a series of nitrostilbene ester compounds using microreactor technology," RSC, vol. 126, pp. 7-10, 2001.

[12] Corning Advanced-Flow Reactors. Controlling Reaction Time and Temperature: Application Note #1, 2018.

[13] P. Beauchamp. "Lecture 2 IR Spectroscopy." Elements of Organic Chemistry, California State Polytechnic University, Pomona, 2010.

[14] A. B. D. Nandiyanto, R. Oktiani, and R. Ragadhita, "How to read and interpret FTIR spectroscope of organic material," *IJoST*, vol. 4, pp. 97-118, 2019.

[15] S. K. A. Mudalip, M. R. A. Bakar, F. Adam, and P. Jamal, "Structures and hydrogen bonding recognition of mefenamic acid form I crystals in mefenamic acid/ethanol solution," *Int J Chem Eng Appl.*, vol. 4, pp. 124-128, June 2013.

[16] J. Lichtenberger, S. C. Hargrove-Leak, and M. D. Amiridis, "In situ FTIR study of the adsorption and reaction of 2′-hydroxyacetophenone and benzaldehyde on MgO," *J. Catal.*, vol. 238, pp. 165-176, February 2006.

[17] J. Chen, X. Jiang, J. Xue, H. Wang, and X. Zheng, "Solvent effect on the initial structural dynamics of benzaldehyde in the $S_3(\pi\pi^*)$ state—resonance Raman spectroscopic study," *J. Raman Spectrosc.*, vol. 50, pp. 684-695, February 2019.

[18] M. Rocha, A. D. Santo, J. M. Arias, D. M. Gil, and A. B. Altabef, "Ab-initio and DFT calculations on molecular structure, NBO, HOMO–LUMO study and a new vibrational analysis of 4-(Dimethylamino) benzaldehyde," *Spectrochim. Acta A Mol. Biomol. Spectrosc.*, vol. 136, pp. 635-643, February 2015.

[19] W. Xie, Y. Ye, A. Shen, L. Zhou, Z. Lou, X. Wang, and J. Hu, "Evaluation of DNA-targeted anti-cancer drugs by Raman spectroscopy," *Vib. Spectrosc.*, vol. 47, pp. 119-123, July 2008.

[20] S. Miljanic, A. Kendel, M. Novak, T. G. Deliqeorqiev, I. Crnolatac, I. Piantanida, and V. Chis, "Distinguishing binding modes of a new phosphonium dye with DNA by surface-enhanced Raman spectroscopy," *RSC Adv.*, vol. 6, pp. 41927-41936, April 2016.

[21] M. Reichel, J. Martens, E. Wollner, L. Huber, A. Kornath, and K. Karaghiosoff, "Synthesis and properties of the fluoromethylating agent (fluoromethyl)triphenylphosphonium iodide," *Eur. J. Inorg. Chem.*, vol. 20, pp. 2530-2534, April 2019.

[22] B. Chakraborty, A. Kostenko, P. W. Menezes, and M. Driess, "A Systems Approach to a One-Pot Electrochemical Wittig Olefination Avoiding the Use of Chemical Reductant or Sacrificial Electrode," *Eur. J. Chem.*, vol. 26, pp. 11829-11834, 2020.

[23] K. Zhang, C. Ma, Y. Zheng, F. Zhou, Y. Xiao, W. Xing, and Y. Hu, "A novel coating of hyperbranched poly(urethane-phosphine oxide) for poly(methyl methacrylate) with high fire safety, excellent adhesion and transparency," *Prog. Org. Coat.*, vol. 161, pp. 1-10, August 2021.

[24] A. Pelusi, Y. Hanawa, H. Araie, I. Suzuki, M. Giordano, and Y. Shiraiwa, "Rapid detection and quantification of haptophyte alkenones by Fourier transform infrared spectroscopy (FTIR)," *Algal Res.*, vol. 19, pp. 48-56, November 2016.

[25] L. Quesada, M. Calero, M. Á. Martín-Lara, A. Pérez, and G. Blázquez, "Production of an Alternative Fuel by Pyrolysis of Plastic Wastes Mixtures," *Energy Fuels*, vol. 34, pp. 1781-1790, January 2020.

[26] F. Cataldo, "Thermal stability, decomposition enthalpy, and Raman spectroscopy of 1-alkene secondary ozonides," *Tetrahedron Lett.*, vol. 56, pp. 994-998, February 2015.

[27] M. Claudino, M. Johansson, and M. Jonsson, "Thiol–ene coupling of 1,2-disubstituted alkene monomers: The kinetic effect of cis/trans-isomer structures," *Eur. Polym. J.*, vol. 46, pp. 2321-2332, December 2010.

7. Supplementary Information

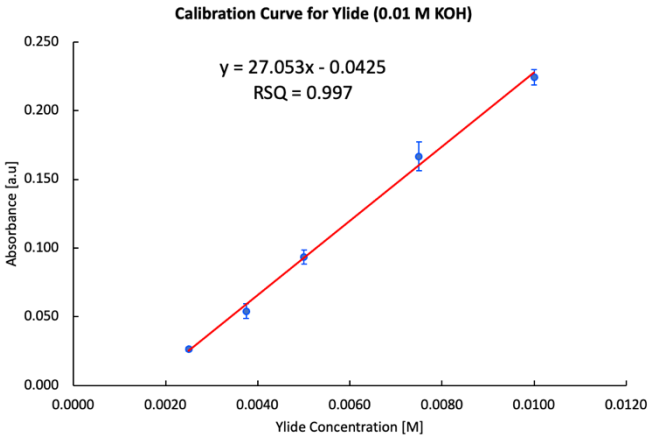

Figure S1. Calibration curve used for kinetic study. 0.01 M KOH was used with various concentrations of NBTP. Error bars are shown using the standard deviation found from the replicate wells.